Fracture Mechanics of Concrete and Concrete Structures - Recent Advances in Fracture Mechanics of Concrete - B. H. Oh, et al.(eds)

Numerical modelling of concrete damage and fracture due to desiccation

H.B. Bian, L. Chen & J.F. Shao
Laboratory of Mechanics of Lille, University of Lille, France

ABSTRACT: The present paper is devoted to numerical study of damage and fracture in cement-based materials subjected to coupled mechanical loads and drying desiccation process. Firstly, a brief summary of basic mechanical behaviour in saturated and unsaturated conditions is given. Based on the experimental evidence, a coupled elastoplastic damage model is proposed in the framework of irreversible thermodynamics. After an analysis of the different failure mechanisms of semi-brittle materials under tensile and compressive stresses as well as in unsaturated condition, a new criterion of damage is proposed taking into account tensile strain generated by saturation gradient. The plastic behaviour of partially saturated materials is described by introducing a generalised concept of effective stress for plastic flow. A particular emphasis is put on the determination of effective stress coefficient from suitable experimental data. Both uniaxial and triaxial compression tests are simulated and a good accordance is obtained between the numerical results and experimental data. In the last part, the constitutive model is implemented in the computer code using extended finite element (XFEM) method. The process of nucleation and propagation of cracks during drying shrinkage is investigated.

1 GENERAL INSTRUCTIONS

In many engineering applications, cement-based materials are subjected not only to mechanical loading, but also to change of saturation condition and to chemical degradation. The durability analysis of concrete structures requires modelling of such multi-physical coupling. A series of experimental data have shown that the mechanical behaviour of cement-based materials is strongly affected by saturation condition (Yurtdas et al. 2004a, b, Gillkey 1937, Mills 1960, Bartlett and MacGregor 1994, Popovics 1986, Burlion et al. 2005). For instance, elastic modulus and mechanical strength can vary with the variation of saturation degree during drying or wetting. Generally, there are two competitive phenomena related to drying effects on mechanical behaviour. Due to the increase of capillary pressure, surface tension or disjoining pressure, the material strength and modulus can locally increase during desiccation. On the other hand, damage by microcracks can be generated by desiccation process, leading to deterioration of material mechanical behaviour. On the other hand, the desiccation induced damage may be resulted by non uniform saturation field at structural scale, and by heterogeneous shrinkage deformation between cement paste and aggregates. In this paper, the emphasis is put on the modelling of structural capillary effects on mechanical behaviour of partially saturated cement-based materials. An elastoplastic damage model is first proposed for cement-based materials in unsaturated condition. A generalized effective stress concept is used for poroplastic coupling. Damage by microcracks is coupled with plastic deformation. The proposed model is applied to a mortar in triaxial compression tests with different degrees of saturation. The elastoplastic damage model is then implemented into a FEM computer code. The mechanical response of a concrete beam in different saturation conditions is analyzed using the proposed model. The model's predictions are in close agreement with experimental data. Based on a criterion related to critical damage density, the passage from diffused damage state to onset of macroscopic crack is described using an extended finite element (XFEM) method. The proposed method is finally applied to modelling of damage and fracture of typical concrete structure components. The damage zone evolution, the localization of damage, the onset and propagation of macrocrack during desiccation process are analyzed.

2 SUMMARY OF EXPERIMENTAL INVESTIGATION

2.1 *Basic mechanical behaviour*

The basic mechanical behaviour of cement-based materials is inherently related to applied stress state. Generally, the typical mechanical response in a triaxial compression tests is composed of different phases: an elastic phase with onset of a small number of microcracks on aggregates – cement paste in-

terfaces; a plastic hardening phase which can be accompanied by quick augmentation of lateral strain and unstable propagation of microcracks until reaching peak stress state, a post-peak softening phase related to strain localization and microcracks coalescence together with rapid reduction of compressive strength and finally a residual phase with a constant residual strength. The relative importance of each phase strongly depends on the value of confining pressure. There is generally a clear transition from brittle to ductile behaviour with increasing confining pressure. Under low confining pressures, the plastic hardening phase is nearly negligible and the material behaviour is essentially controlled by damage by microcracks. The residual strength is close to zero. Under higher confining pressures, the plastic deformation phase is the dominant mechanism compared with damage. When the confining pressure is high enough, the post-peak phase may disappear and we have a fully ductile plastic response usually accompanied by important volumetric compaction. On the other hand, under direct tensile stress, the mechanical response is typically brittle in nature; with an elastic phase until the peak stress followed by drastic material softening before macroscopic fracture. Therefore, in order to describe mechanical responses of cement-based materials under multi-axial conditions, it is proposed here to formulate an elastoplastic model coupled with induced damage.

2.2 *Mechanical behaviour under partially saturated conditions*

Extensive experimental investigations have been carried out to study various phenomena and influences on mechanical behaviours related to desiccation process. It is revealed that, the saturation degree has a great influence on the mechanical behaviour of cement-based material. The influence exists in both elastic and plastic domains. A large review of the experimental studies can be found in Yurtdas (2003). Figure 1 presents the evolution of compressive strength of samples in different saturation conditions during triaxial compression tests performed in a normalized mortar. We can observe an increase of about 29% in failure stress after 162 days drying. Similar results are also reported on other cement-based materials (Burlion et al. 2005, Popovics 1986 just to mention a few). Concerning physical origins of mechanical strength increase, discussions are still open. However, among various phenomena, the most commonly one is the capillary pressure which leads to an additional confining effect on material skeleton. As this effect can be easily quantified from laboratory tests, it will be taken as the main responsible of drying effects in this work.

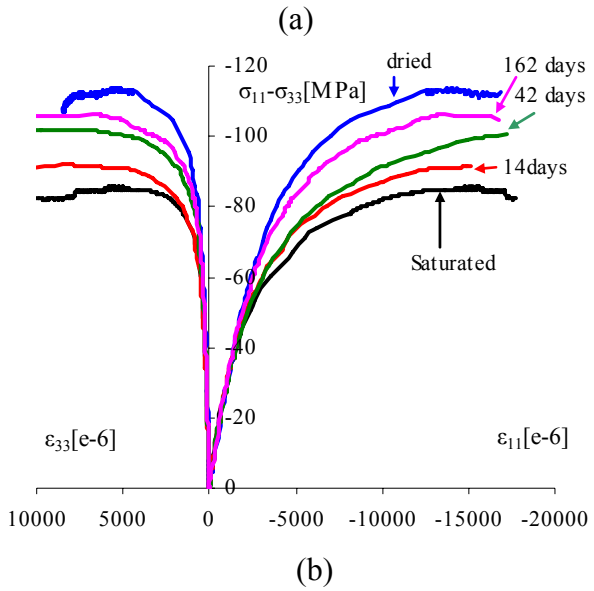

Figure 1. Evolution of the compressive strength of a normalized mortar in triaxial compression tests after different drying periods (Yurtdas 2003).

3 FORMULATION OF CONSTITUTIVE MODEL

Based on the experimental investigations, a coupled elastoplastic model is proposed for the description of mechanical behaviour of the cement-based material. In this work, the assumption of small strains is adopted, so in the isothermal conditions, the state variables are constituted of total strain tensor $\boldsymbol{\varepsilon}$, scalar damage variable ω, plastic strain $\boldsymbol{\varepsilon}^p$ and internal variable for plastic hardening γ_p. As classically, the total strain could be decomposed into an elastic part $\boldsymbol{\varepsilon}^e$ and a plastic part $\boldsymbol{\varepsilon}^p$, expressed as following:

$$\boldsymbol{\varepsilon} = \boldsymbol{\varepsilon}^e + \boldsymbol{\varepsilon}^p, \mathrm{d}\boldsymbol{\varepsilon} = \mathrm{d}\boldsymbol{\varepsilon}^e + \mathrm{d}\boldsymbol{\varepsilon}^p \tag{1}$$

Based on thermodynamic theory, it is assumed that the thermodynamic potential ψ can be expressed by (Chen 2007, Shao 2006):

$$\psi = \frac{1}{2}(\boldsymbol{\varepsilon} - \boldsymbol{\varepsilon}^p) : \mathbb{C}(\omega) : (\boldsymbol{\varepsilon} - \boldsymbol{\varepsilon}^p) + \psi_p(\gamma_p, \omega) \tag{2}$$

$\mathbb{C}(\omega)$ is the fourth order elastic stiffness tensor of damaged material, and the function ψ_p represents the locked plastic energy for plastic hardening of damaged material. The standard derivation of the thermodynamic potential yields the state Equation:

$$\boldsymbol{\sigma} = \frac{\partial \psi}{\partial \boldsymbol{\varepsilon}^e} = \mathbb{C}(\omega) : (\boldsymbol{\varepsilon} - \boldsymbol{\varepsilon}^p) \tag{3}$$

For the isotropic material, we have the following expression of effective elastic stiffness tensor:

$$\mathbb{C}(\omega) = 3k(\omega)\mathbb{J} + 2\mu(\omega)\mathbb{K} \quad (4)$$

$k(\omega)$ is the bulk modulus of the damaged materials and $\mu(\omega)$ represents the shear modulus. The degradation of elastic properties caused by damage was taken into account by the following form:

$$k(\omega) = k_0\left[1 - H(\varepsilon_v)\omega\right],\ \mu(\omega) = \mu_0(1-\omega) \quad (5)$$

k_0 and μ_0 is respectively the initial drained bulk and shear modulus of intact material. $H(\varepsilon_v)$ is the Heaviside function of volumetric strain ε_v in order to account for unilateral effect on bulk modulus.

It is here assumed that porous materials are saturated by a liquid phase and a gas mixture. The elastic behaviour of partially saturated materials will depend on pressures of different fluid phases. Based on the previous works by Coussy et al. (1998) and Coussy (2004), the effects of liquid and gas pressures are characterized by an equivalent pore pressure, π, defined as:

$$d\pi = dp_g - S_l(p_{cp})dp_{cp}\ ;\ \pi = \int d\pi \quad (6)$$

p_g and p_l is respectively gas and liquid pressure, $p_{cp} = p_g - p_l$ is capillary pressure and S_l denotes water saturation. Using this equivalent pore pressure, the elastic constitutive relations are expressed as:

$$\sigma_{ij} = \left(k_b(\omega) - \frac{2}{3}\mu(\omega)\right)tr(\varepsilon^e)\delta_{ij} + 2\mu(\omega)\varepsilon^e_{ij} - b(\omega)\pi\delta_{ij} \quad (7)$$

$b(\omega)$ is the Biot's coefficient, which also depends on the damage variable.

3.1 *Plastic modelling*

As mentioned above, the mechanical behaviour of cement-based material is very sensitive to water saturation degree in partially saturated condition. In the general framework of thermodynamics, the plastic deformation of porous materials is controlled by applied stresses and fluid pressures. The plastic yield criterion should be a function of all independent force variables. However, it is very difficult to experimentally determine such general criterion due to technical limitation. One simplified approach consists in extending plastic criteria of dry materials to partially saturated conditions by using relevant effective stress concept according to the stress equivalence principle. Although the existence of such effective stresses is theoretically not proved, this concept provides an efficient tool for plastic and damage modelling in saturated and unsaturated materials. This concept is adopted and extended here. Adopting the equivalent pore pressure defined above, we propose to introduce the following effective stress tensor for plastic modelling of partially saturated materials:

$$\sigma^{pl}_{ij} = \sigma_{ij} + \beta(\sigma, S_l)\pi\delta_{ij} \quad (8)$$

The generalized effective stress coefficient β characterizes effects of the equivalent pore pressure on plastic deformation. Its value should depend not only on applied stress state but also on saturation degree. The determination of β is discussed in next section. Based on some previous work, the following function is proposed as plastic function with the plastic effective stresses defined in (8):

$$f_p(\sigma_{ij}, \eta) = \tilde{q} - g(\tilde{\theta})\eta(\gamma)P_a(C_s + \frac{\tilde{p}}{P_a})^m = 0 \quad (9)$$

where

$$\tilde{p} = -\frac{\tilde{\sigma}_{kk}}{3}, \tilde{q} = \sqrt{3J_2}, J_2 = \frac{1}{2}s_{ij}s_{ij}, s_{ij} = \tilde{\sigma}_{ij} - \frac{\tilde{\sigma}_{kk}}{3}\delta_{ij}$$

The parameter C_s represents the hydrostatic tensile strength corresponding to the intersection of the failure surface with the mean stress axis. The function $g(\tilde{\theta})$ allows accounting for the dependency of yield function on the Lode angle in the deviatoric plane. Various expressions of $g(\tilde{\theta})$ have been proposed in literature for geomaterials. The emphasis of this work is on the poroplastic modelling of unsaturated materials, the expression of $g(\tilde{\theta})$ is here simplified and taken to be $g(\tilde{\theta}) = 1$. As a non linear yield surface is used here, two parameters (m and η) are used to determine the shape and position of the yield surface. Given a set of values of these two parameters, one can determine the material cohesion. And note that the frictional angle in such non linear criterion is not constant but depends on the mean stress ($\tilde{p}$). Further, for $m = 1$ and $g(\tilde{\theta}) = 1$, the yield function reduces to the classical Drucker-Prager criterion.

The plastic hardening is characterized by the variation of the coefficient η, as a function of the generalized plastic shear strain noted by γ_p; while the value of parameter (m) is assumed constant. Considering that the softening of mortar is generally induced by the initiation and propagation of the microcracks, the plastic hardening law contains an increasing function of the internal hardening variable γ_p but also a decreasing function of the damage

variable ω. Based on the experimental data in triaxial compression tests, the following function is proposed:

$$\eta(\gamma_p)= (1-\omega)\left[\eta_0+(\eta_m-\eta_0)\frac{\gamma_p}{b_1+\gamma_p}\right] \quad (10)$$

The parameter b_1 controls the plastic hardening speed; η_0 and η_m present respectively the initial yield threshold and ultimate value of frictional coefficient. The internal hardening variable is taken as the generalized plastic distortion defined by:

$$d\gamma_p=\frac{\sqrt{\frac{2}{3}de_{ij}^p de_{ij}^p}}{\chi_p}, de_{ij}^p=d\varepsilon_{ij}^p-\frac{d\varepsilon_{kk}^p}{3}\delta_{ij} \quad (11)$$

The normalizing coefficient χ_p is introduced here to take into account the dependence of plastic hardening ratio on confining pressure.

In order to better describe the volumetric strain during plastic flow, based on the experimental evidence and inspired by the works by Pietruszczak et al. (1988), the following non-associated rule was proposed as the plastic potential function.

$$Q=\tilde{q}+\mu_c g(\tilde{\theta})(\tilde{p}+P_aC_s)\ln\left(\frac{\tilde{p}+P_aC_s}{\bar{p}}\right)=0 \quad (12)$$

The coefficient $\bar{p}$ corresponds to the intersection point between the plastic potential surface and the axis $(p+P_aC_s)>0$. The coefficient μ_c represents the ratio $\tilde{q}/g(\theta)(\tilde{p}+P_aC_s)$ at the point for which $\partial Q/\partial\tilde{p}=0$.

3.2 *Damage modelling*

In the framework of thermodynamics for time independent damage process, the damage evolution is determined by a damage criterion which is a function of conjugate damage force.

As mentioned above, the failure mechanisms are different in compressive and tensile stress state for cement-based material. In compression condition, the damage is mainly induced by the frictional sliding along the microcracks which can be considered as the plastic deformation. On the contrary, in tensile stress condition, the damage evolution is mainly related to the development of opened microcracks which is exhibited as positive strain. So the damage evolution laws should be considered separately. In the present work, we assume that the damage value is composed of a compressive part and a tensile part. Based on the analysis above, the compressive damage criterion is a function of the compressive damage conjugate force Y_c^ω, and the tensile damage criterion is a function of the positive strain. Based on some previous works, the following function is proposed:

$$Y_c^\omega=\max(\gamma_p,Y_{c,0}^\omega) \quad (13)$$

$$Y_t^\omega=\max(\varepsilon_{eq},Y_{t,0}^\omega) \quad (14)$$

$$\varepsilon_{eq}=\sqrt{\sum_{i=1}^{3}\langle\varepsilon_i\rangle^2}+\sqrt{\sum_{i=1}^{3}\left\langle\varepsilon_i-\frac{b}{3k_0}\pi\right\rangle^2} \quad (15)$$

here, the variable ε_{eq} is composed of two parts, the first part is the positive strain, and the second part represents the influence of the gradient of equivalent pore pressure on the evolution of damage due to desiccation process.

$$\omega_c=\omega_{cc}-\omega_{cc}\frac{1}{\exp\left[B_c\left(Y_c^\omega-Y_{c,0}^\omega\right)\right]} \quad (16)$$

$$\omega_t=\omega_{ct}-\omega_{ct}\frac{1}{\exp\left[B_t\left(Y_t^\omega-Y_{t,0}^\omega\right)\right]} \quad (17)$$

ω_t and ω_c denote respectively the tensile and compressive part of the damage value. The total damage is composed of these two parts:

$$\omega=(1-\alpha_t)\omega_c+\alpha_t\omega_t \quad (18)$$

The coefficient α_t is determined by:

$$\alpha_t=\frac{\left\|\bar{\bar{\sigma}}^+\right\|}{\left\|\bar{\bar{\sigma}}\right\|} \quad (19)$$

$\bar{\bar{\sigma}}^+$ is the positive cone of the applied stress tensor.

4 NUMERICAL SIMULATIONS

In order to verify the capacity of the proposed model, the laboratory test performed by Yurtdas (2003) are simulated in this part. Firstly, we present the determination of model's parameters.

4.1 *Identification of model's parameters*

The plastic hardening law is determined by drawing the frictional coefficient $\eta(\gamma_p)$ with the generalized plastic shear strain γ_p, which is calculated on unloading paths. The parameter μ_c defines the slope of transition boundary between volumetric compressibility to dilatancy; it is then identified from the points on volumetric strain curves. The asymptotic

damage value, ω_{cc}, can be identified from the ratio between peak stress and residual strength in post failure regime. For the sake of simplicity, B_c is determined by fitting post peak stress strain curves. The tensile damage parameters ω_t, B_t and $Y_{t,0}^{\omega}$ can be determined by fitting the direct tension test.

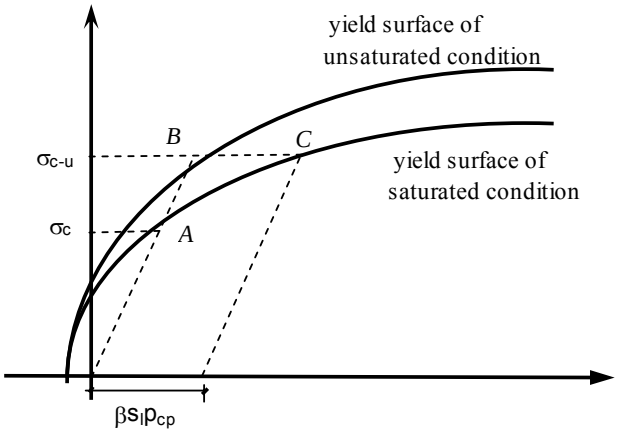

Figure 2. Illustration of procedure for the determination of effective stress coefficient in unsaturated conditions.

In the poroplastic modelling proposed here, the effective stress coefficient for plastic deformation, β, plays an essential role in poroplastic coupling. In unsaturated conditions, the following procedure is proposed to determine the variation of β as a function of saturation. The failure surface of saturated material is first determined as the reference state. Then for a given unsaturated state, the uniaxial compression strength is measured and compared with that of saturated material. The difference between the two values is used to evaluate the quantity, $\beta S_l p_{cp}$. As the capillary pressure is related to isothermal sorption – desorption curve, the corresponding value of β is then obtained. This procedure is illustrated in Figure 2.

Further, due to the lack of relevant experimental data and for the sake of simplicity, it is assumed that the parameter β is not affected by material damage. By using this procedure for different confining pressure, the influence of this last one can also be identified. For the mortar studied here, only two confining pressures are available, namely 0 and 15MPa. Therefore, it appears difficult to give a general description of confining pressure effect. Only the following relations are obtained respectively for the two confining pressures, as shown in Figure 3. The values of parameters used in the numerical modelling are given in Table 1.

$$\begin{cases} \beta = (1-a_0)\exp(b(S_l-1))+a_0 \\ a_0 = 0.2,\ b = 14,\ \text{for } p_c = 0\text{MPa} \\ a_0 = 0.25,\ b = 14,\ \text{for } p_c = 15\text{MPa} \end{cases} \quad (20)$$

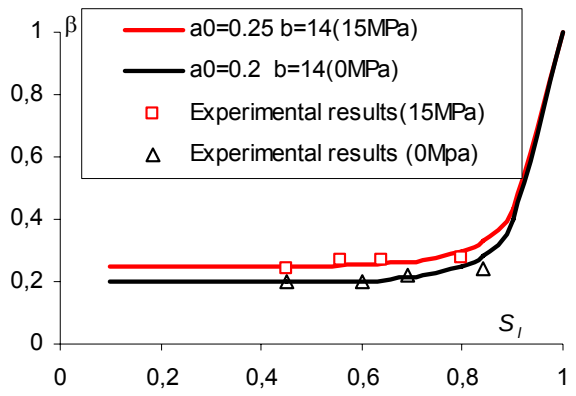

Figure 3. Variations of plastic effective stress coefficient with saturation degree for two different confining pressures.

Table 1. Representatives values of parameters in the model.

Class	name
Elastic constant	E=36400MPa , ν=0.19
Plastic parameters	C_s =19.0, m =1, η_0=0.6, η_m =1.42, b_l=3.0×10^{-5} ,μ=1.5
Damage characterization	$Y_{c,0}^{\omega}$ =0.0, B_c =300.0, ω_c =0.2, ω_t = 0.99 , B_t = 2500 , $Y_{t,0}^{\omega}$ = 0

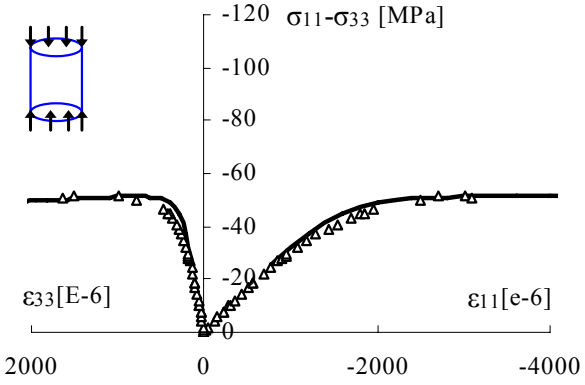

(a)

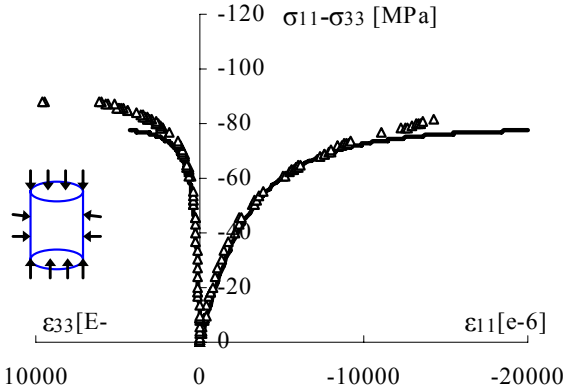

(b)

Figure 4. Comparison between simulations (continuous lines) and test data (points) in the case of (a) uniaxial; (b) triaxial compression tests for saturated samples.

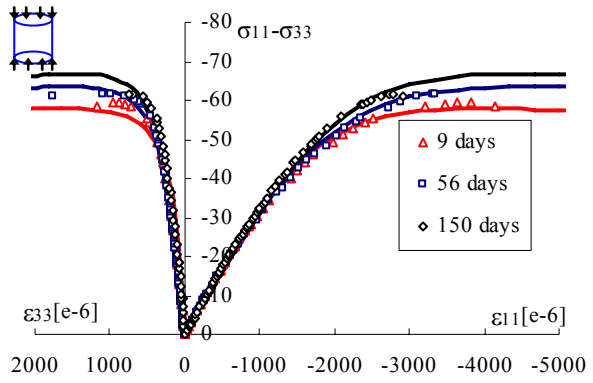

(a)

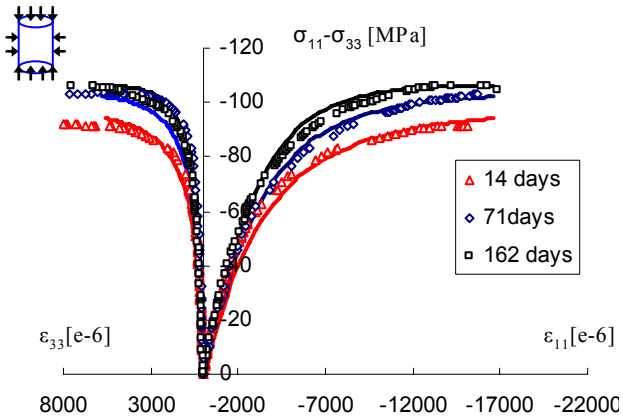

(b)

Figure 5. Stress-strain curves of samples with different periods of desiccation – comparisons between model's predictions (lines) and experimental data (symbols) (a) uniaxial test (b) triaxial compression tests (Pc=15MPa).

Using these parameters, numerical simulation of laboratory tests has been performed. Figure 4 shows the strain evolution for triaxial compression tests under different confining pressures. We can notice than the main mechanical behaviours are well reproduced by the proposed model, including the softening behaviour due to progressive growth of microcracks.

Stress-strain curves in compression tests are presented in Figure 5. It can be noticed that the influence of desiccation is clearly reproduced. There is a good correlation between numerical predictions and experimental data.

5 THE EXTENDED FINIT ELEMENT METHOD

In fact for the desiccation process in concrete structure, two distinct phases can be identified. The first stage involves the onset and the propagation of microcracks in cement matrix and in the interface of cement and aggregates. Later in the further desiccation process, the microcracks localize and nucleate to macrocracks, and displacement discontinuities develop in material. For the first stage, the microcracks are represented by damage, and mechanical behavior has been described by the constitutive model presented in the previous section. However, for the second stage of failure, the appearance of macrocracks (moving discrete surfaces, across which displacement are discontinuous) causes much problem for the traditional numerical method. The extended finite element method (XFEM), which is firstly used as a method for analyzing crack growth without remeshing by employing enriched functions to simulate the discontinuity with a fixed mesh (Moës et al. 1999), is adopted in current study.

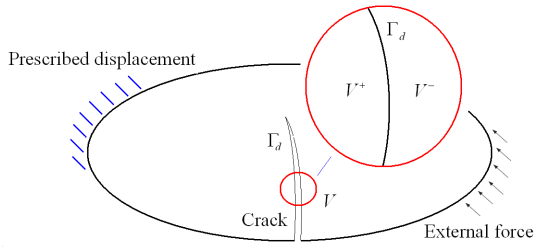

Figure 6. Concrete materials damaged by a macrocrack.

We consider a representative volume element V of concrete which has been crossed by the crack Γ_d depicted in Figure 6. The crack has a direction from the end to its head (crack tip). The crack splits the volume into two parts: V^+ locates at left side of crack and V^- at right side ($V = V^+ \bigcup V^-$). The displacement field u can be decomposed into two parts: a continuous part for classical finite element method u_n and a discontinuous part for the enriched nodes displacement u_r, as shown in the following:

$$u(x,t) = u_n(x,t) + H(x)u_r(x,t) \tag{21}$$

Both the two displacement fields u_n and u_r are continuous function on the represented volume element V. $H(x)$ is the Heaviside step function as:

$$H(x) = \begin{cases} +1 & \text{if } x \in V^+ \\ -1 & \text{if } x \in V^- \end{cases} \tag{22}$$

The XFEM are similar to that of classical FEM. The only difference lies on the macrocracks onset and propagation.

Physically, the macrocracks are the result of the coalescence of microcracks, so it was supposed that the onset of the crack is controlled by the damage. When the damage arrives at certain level, the macrocracks are initiated. Firstly the simple traction test of the concrete was simulated by using the damage model proposed in the previous section. The results are given in Figure 7 (the variation of the axial stress and the damage in function of the axial deformation). The axial stress is normalized by its peak value. It is supposed that, when the axial stress ar-

rives at its peak value, the macrocracks appear, and the material could support no more traction force. At this moment, the damage is about 0.4, this value was then set as the threshold for the onset/propagation of the fractures. While for the crack propagation direction: since the crack tip is not located exactly at a gauss point (the discontinuity is independent of mesh), the local stress field cannot be relied upon to accurately yield the correct normal vector to a fracture. To overcome this difficulty, the average stress criterion proposed by Wells et al. (Wells et al. 2002) is employed. It is supposed that the principal axis of the averaged stress tensor corresponding to the maximum principal stress, and is taken as the normal vector of the crack extension.

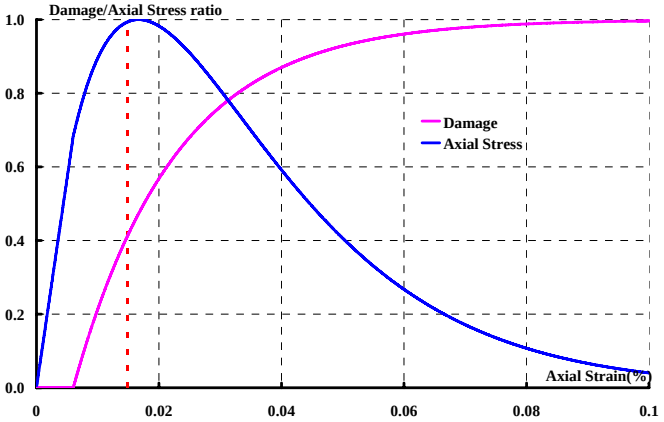

Figure 7. Uniaxial traction test of concrete.

6 APPLICATION

In this section, we present a numerical example of crack onset/propagation under desiccation and mechanical loading based on the framework of XFEM in 2D (with the assumptions of plane strain). The mechanical behavior of cement based material is described by the numerical model proposed in present work. We consider one concrete beam with the length as 1.5 meters and 0.5metre in height. In the length direction, there are totally 61 elements, while in the vertical direction there are 50 elements. The 4-node quadrilateral element is used in this study. The two corners at the bottom of the beam are supported with two simple articulations (the vertical displacement is blocked); while at the upper side of the beam, the horizontal displacements of two centre points are fixed. The concrete beam is supposed as initially saturated. And then the bottom side of beam is submitted to the desiccation loading by the ventilation with a relative humidity of 87% during one year.

Due to ventilation, the concrete beam is under the desiccation loading; as a consequence, the volumetric shrinkage was developed in concrete matrix. Because of the structure effects, the damage increase rapidly in the lower centre of the beam. The distributions of damage at different stage are given in Figure 8.

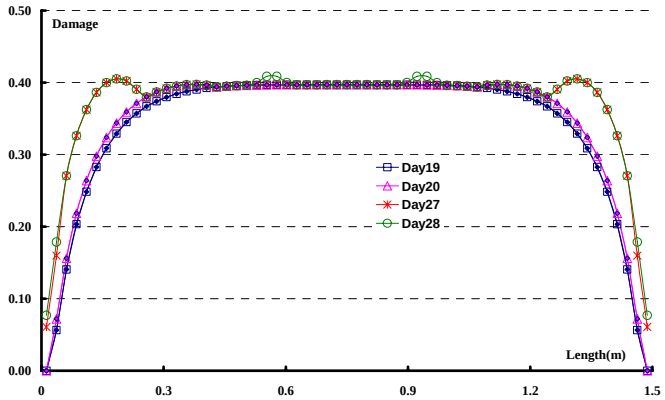

Figure 8. Distribution of damage at the bottom of the beam at different time of desiccation.

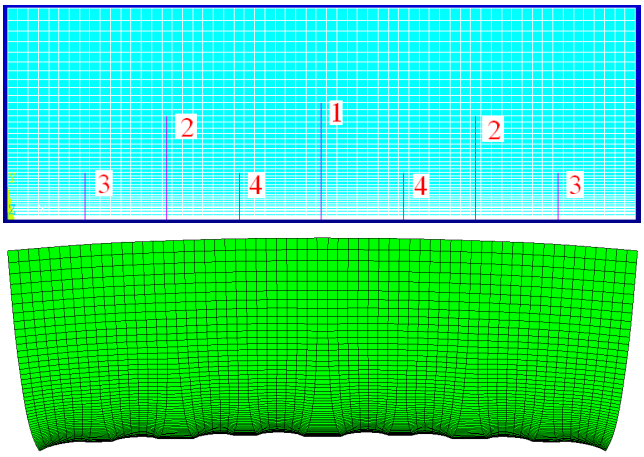

Figure 9. The distribution of cracks in concrete beam during desiccation and the corresponded deformed mesh.

It can be seen that: at the beginning, the damage is generated at the lower centre of the beam, and the distribution is quasi homogeneous between 0.4 and 1.1meter. The maximum value however is at the centre of beam. The first macrocrack is then initiated at about 19 days of loading, while the equivalent pore pressure is about 6.7MPa. With the progress of desiccation, the damage in the centre of beam is almost constant. This, however, is reasonable. Because of the first crack, the structure rigidity decrease, especially at the approximation of the first fracture, so even with the increase of desiccation loading, the damage in this region has no significant increase. While at two sides of the first crack (far away from the first crack), the damage increase slightly with the desiccation procedure, and then two cracks (as marked as crack 2 in Fig. 9) appear. Thus, the beam was divided into 4 parts. However, the two segments at two ends of concrete beam are longer than those two insider segments. With the increase of time, the damage in the two long segments increase rapidly, and the two third cracks appears (as marked as crack 3 in Fig. 9), while the damage in

centre part rests as constant until the appearance of two further cracks. At last, the damage in two centre segments has a sudden increase, which results to two small cracks (crack 4 as marked in Fig. 9). And then the damage rests quasi constant during one year desiccation. The onset times for each fracture are respectively 19day, 20day, 27 and 28 day.

7 CONCLUSIONS

Based on the evidence of experimental data, a coupled elastoplastic damage model is proposed for the cement-based material. By introducing the concept of plastic effective stress, the model is extended to the partially saturated conditions. The simulation of laboratory test both in saturated and unsaturated are performed in which a good agreement with experimental data is obtained. The main hydromechanical behaviors such as plastic deformation, evolution of damage, pressure sensitivity, and softening behavior are well reproduced by the model.

And then based on the framework of XFEM, the full failure procedure of concrete beam under desiccation loading is studied. The onset and the propagation of the fractures are controlled by the level of damage, and the direction of fractures is derived from the average stress tensor. The total schema gives a full continuous analysis for the concrete beam subjected to desiccation loading, and represents well the total failure process of material due to desiccation process.

REFERENCES

Barlett, F.M. &MacGregor, J.G. 1994. Effect of moisture condition on concrete core strengths. *ACI Mater. J.* 91(3): 227-236.

Burlion, N., Bourgeois F.& Shao, J.F. 2005. Effects of desiccation on mechanical behaviour of concrete. Cement & Concrete Composites 27:367–379

Chen,D. 2003. Modelisation du comportement hydermecanique d'un mortier sous compression et dessiccation. Doctoral thesis, Univ. des Science et technologies de Lille, France

Coussy, O., Eymard, R. & Lassabatére, T. 1998. Constitutive modelling of unsaturated drying deformable materials. *Journal of Engineering Mechanics-ASCE* 124(6):658–667.

Coussy, O.2004. Poromechanics. *John Wiley & Sons*.

Gilkey, H.J. 1937. The moist curing of concrete. Eng. *News-Rec.* 119(10):630-633.

Mills, R.H.1960. Strength-maturity relationship for concrete which is allowed to dry. *RILEM Int. Symp. On Concrete and Reinforced Concrete in Hot Country,* Haîfa, Israël.

Möes, N., Dolbow J.& Belytschko T., 1999, Finite element method for crack growth without remeshing, *International journal for numerical methods in engineering* 46, 131-150.

Pietruseczak, S. & Jiang, J. & Mirza, F.A. 1988. An elastoplastic constitutive model for concrete. *Int. J. Solid and Structures* 24(7): 705-722.

Popovics, S. 1986. Effect of curing method and moisture condition on compressive strength of concrete. *ACI J.,* 83(4)*:* 650-657.

Shao, J.F., Jia, Y., Kondo, D. &Chiarelli, A.S. 2006. A coupled elastoplastic damage model for semi-brittle materials and extension to unsaturated conditions. *Mechanics of Materials* 38:218–23.

Wells, G. N. Sluys L. J.& de Borst R. 2002. Simulating the propagation of displacement discontinuities in a regularized strain-softening medium, *International journal for numerical methods in engineering* 53,1235–1256.

Yurtdas ,I. &Burlion, N. &Skoczylas , F . 2004b. Triaxial mechanical behavior of mortar: Effect of drying. *Cem. Concr. Res.*34(7):1131-1143.

Yurtdas ,I.,Burlion, N. & Skoczylas, F . 2004a. Experimental characterization of the drying effect on uniaxial mechanical behavior of mortar. *Mater. Struct.* 37(3),170-176.

Yurtdas,I.2003. Couplage comportement mécanique et dessiccation des matétiaux à matrice cimentaire :étude expérimentale sur mortier. Doctoral thesis ,Univ . des Science et thchnologies de Lille et Ecole Centrale de Lille, France.